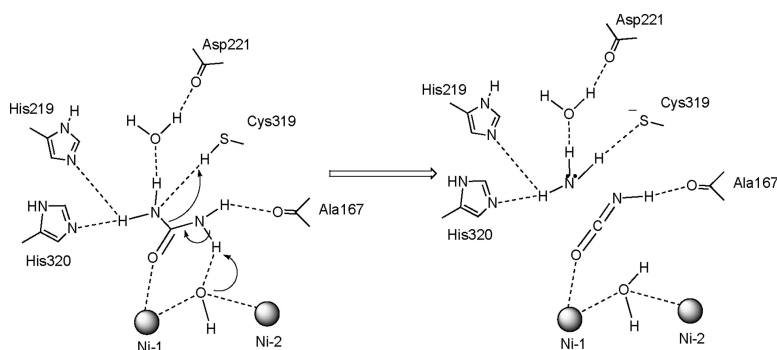


Enzymatic Catalysis of Urea Decomposition: Elimination or Hydrolysis?

Guillermina Estiu, and Kenneth M. Merz

J. Am. Chem. Soc., **2004**, 126 (38), 11832-11842 • DOI: 10.1021/ja047934y • Publication Date (Web): 03 September 2004

Downloaded from <http://pubs.acs.org> on April 1, 2009



More About This Article

Additional resources and features associated with this article are available within the HTML version:

- Supporting Information
- Links to the 3 articles that cite this article, as of the time of this article download
- Access to high resolution figures
- Links to articles and content related to this article
- Copyright permission to reproduce figures and/or text from this article

[View the Full Text HTML](#)

Enzymatic Catalysis of Urea Decomposition: Elimination or Hydrolysis?

Guillermina Estiu and Kenneth M. Merz, Jr.*

Contribution from the Department of Chemistry, The Pennsylvania State University,
152 Davey Laboratory, University Park, Pennsylvania 16802-6300

Received April 9, 2004; E-mail: merz@psu.edu

Abstract: We present a high-level quantum chemical study of possible reaction mechanisms associated with the catalytic decomposition of urea by a bioinorganic mimetic of the dinickel active site of urease. We chose the phthalazine–dinickel complexes of Lippard and co-workers, because these mimetics have been shown to hydrolytically degrade urea. High-level quantum chemical methodologies were utilized to identify stable intermediates and transition-state structures along several possible reaction pathways. The computed results were then used to further analyze what may occur in the active site of urease. Valuable information on the latter has been extracted from experimental data, computational approaches, and unpublished molecular dynamics simulations. On the basis of these comparative studies, we propose that both the elimination and hydrolytic pathways may compete for urea decomposition in the active site of urease.

Introduction

Dinuclear metallohydrolases are an important group of metalloenzymes, which catalyze the hydrolysis of a range of peptide and phosphate ester bonds. They include the amidohydrolases, amidinohydrolases, and peptide hydrolases.¹ They are characterized by the presence of two metal ions in the active site (e.g., Zn(II), Ni(II), and Co(II)), which are complexed by one or more bridging ligands that are frequently involved in the catalytic mechanism. The number of X-ray crystal structures for this class of enzymes is rapidly growing and include penicillin amidohydrolases, ureases, asparaginases, and creatinine amidinohydrolases among others.^{2–5} Nevertheless the mechanism involved in their catalytic hydrolysis of various substrates is still a matter of discussion. Most of the recent advances in our mechanistic understanding of this class of enzymes have been mainly grounded in the study of urea amidohydrolase.^{6–14}

Urea amidohydrolase (urease) is a nickel-dependent enzyme, present in various plants and microorganisms, that catalyzes the hydrolysis of urea to ammonia and carbon dioxide (and small amides to the corresponding carboxylic acids), which causes an abrupt increase of pH.^{6,15} It plays important roles in the nitrogen metabolism of plants and microbes. The widespread activity of urease in soil, present both in living ureolytic bacteria and as extracellular urease, can severely decrease the efficiency of urea as a soil fertilizer and simultaneously release large quantities of toxic ammonia. Urease activity also constitutes a virulence factor in human and animal infections of the urinary and gastrointestinal tracts. In particular, *Helicobacter pylori*,^{16–18} a gram negative microaerophilic bacterium first isolated in the stomach of patients with gastritis and peptic ulcers, has been associated with several gastroduodenal diseases including cancer and produces a large amount of urease, which is believed to play an essential role in facilitating bacterial survival.¹⁹

The initial X-ray crystal structures of the native urease from *Klebsiella aerogenes*^{3,6} and *Bacillus pasteurii*,^{7,20} as well as subsequent crystallographic work based on mutagenesis experiments,^{11–13,21} have provided detailed insights into the active site structure and have identified a pair of nonequivalent Ni atoms at a Ni–Ni separation close to 3.5 Å. Each Ni ion is coordinated to two histidine residues from the protein, and a carbamylated lysine bridges the two metal atoms (Figure 1). The second nickel ion is also ligated by an aspartate residue.

- (1) Wilcox, D. E. *Chem. Rev.* **1996**, *96*, 2435–2458.
- (2) Strater, N.; Lipscomb, W. N. *Biochemistry* **1995**, *34*, 14792–14800.
- (3) Jabri, E.; Carr, M. B.; Hausinger, R. P.; Karplus, P. A. *Science* **1995**, *268*, 998–1004.
- (4) Roderick, S. L.; Matthews, B. W. *Biochemistry* **1993**, *32*, 3907–3912.
- (5) Kanyo, Z. F.; Scolnick, L. R.; Ash, D. E.; Christianson, D. W. *Nature* **1996**, *383*, 554–557.
- (6) Karplus, P. A.; Pearson, M. A.; Hausinger, R. P. *Acc. Chem. Res.* **1997**, *30*, 330–337.
- (7) Benini, S.; Ciurli, S.; Rypniewski, W. R.; Wilson, K. S.; Mangani, S. *Acta Crystallogr., Sect. D: Biol. Crystallogr.* **1998**, *54*, 409–412.
- (8) Benini, S.; Rypniewski, W. R.; Wilson, K. S.; Miletti, S.; Ciurli, S.; Mangani, S. *Struct. Fold. Des.* **1999**, *7*, 205–216.
- (9) Benini, S.; Rypniewski, W. R.; Wilson, K. S.; Ciurli, S.; Mangani, S. *J. Biol. Inorg. Chem.* **2001**, *6*, 778–790.
- (10) Musiani, F.; Arnolfi, E.; Casadio, R.; Ciurli, S. *J. Biol. Inorg. Chem.* **2001**, *6*, 300–314.
- (11) Pearson, M. A.; Michel, L. O.; Hausinger, R. P.; Karplus, P. A. *Biochemistry* **1997**, *36*, 8164–8172.
- (12) Pearson, M. A.; Prk, I.-S.; Schaller, R. A.; Michel, L. O.; Karplus, P. A.; Hausinger, R. P. *Biochemistry* **2000**, *39*, 8575–8584.
- (13) Pearson, M. A.; Schaller, R. A.; Michel, L. O.; Karplus, P. A.; Hausinger, R. P. *Biochemistry* **1998**, *37*, 6214–6220.
- (14) Todd, M. J.; Hausinger, R. P. *Biochemistry* **2000**, *39*, 5389–5396.

- (15) Zerner, B. *Biorg. Chem.* **1991**, *19*, 116–131.
- (16) Covacci, A.; Telford, J. L.; Del Giudice, G.; Parsonnet, J.; Rappuoli, R. *Science* **1999**, *284*, 1328–1333.
- (17) Dunn, B. E.; Cohen, H.; Blaser, M. J. *Clin. Microbiol. Rev.* **1997**, *10*, 720–741.
- (18) Dunn, B. E.; Grutter, M. G. *Nat. Struct. Biol.* **2001**, *8*, 480–482.
- (19) Ha, N. C.; Oh, S. T.; Sung, J. Y.; Cha, K. A.; Lee, M. H.; Oh, B. H. *Nat. Struct. Biol.* **2001**, *8*, 505–509.
- (20) Benini, S.; Rypniewski, W. R.; Wilson, K. S.; Ciurli, S.; Mangani, S. *J. Biol. Inorg. Chem.* **1998**, *3*, 268–263.
- (21) Jabri, E.; Karplus, P. A. *Biochemistry* **1996**, *35*, 10616–10626.

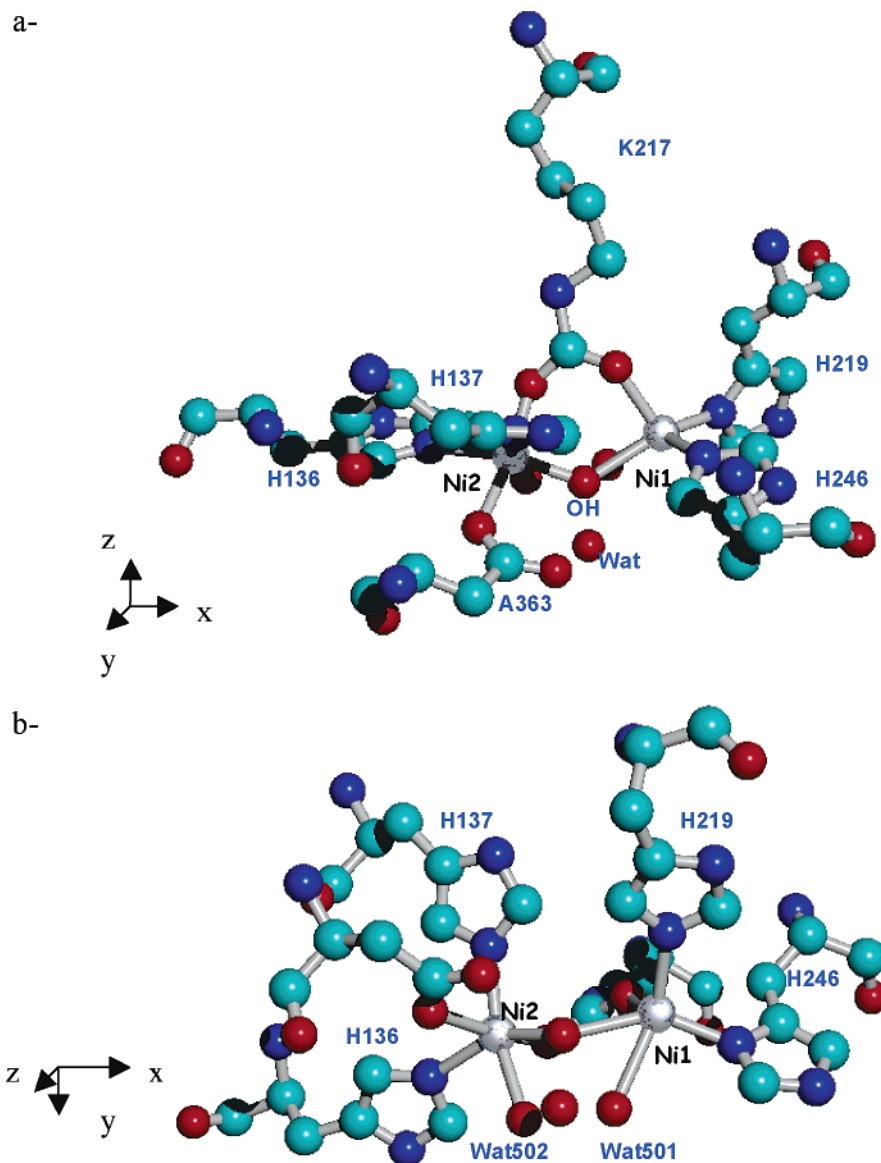


Figure 1. Active site of the dinickel urease enzyme from *Bacillus pasteurii* (PDB code 2UBP) determined by X-ray crystallography. Panels a and b show two views of the active site.

Two terminally coordinated water molecules and one bridging water molecule or hydroxide ion complete the coordination sphere of the metal ions, resulting in a distorted square-pyramidal environment for Ni1 and a pseudooctahedral one for Ni2.^{6,22} These structural properties strongly suggest different mechanistic roles for the two metal atoms. There is general agreement on the role of the low coordinated Ni center, which is likely involved in binding urea through the carbonyl oxygen of urea. The second Ni atom has been suggested to help the catalytic pathway in different ways, either providing a solvent nucleophile or coordinating an amino group of the urea molecule. The second possibility became generally accepted, after the crystal structure of the DAP-inhibited (DAP = diamidophosphate) urease was reported, which showed a bidentate coordination of DAP that displaced the nickel-coordinated water molecules.⁹ Extrapolating this model to urea, one can predict that the carbonyl group would bind to the most electrophilic Ni1 site, while one of the amide nitrogens would

coordinate to Ni2. This coordination mode favors the attack of the bridging OH on the carbonyl C atom, stabilizing a tetrahedral intermediate that is thought to be involved in the reaction path. The present mechanistic discussion centers on how the intermediate is stabilized, which largely relates to the protonation state of nearby residues that are supposed to be involved in the catalytic pathway.^{6,9} For example the role of His320, which has been identified as a key residue for catalysis, is not well-understood.⁶

Understanding the mode of urea bonding to urease is an important issue, because it could facilitate the design of inhibitors that are capable of blocking the activity of the enzyme. Recent calculations have identified urease as one of the most proficient enzymes.²³ This fact increases the relevance of this research, as the proficiency of an enzyme is related to the stability of the transition-state structure involved in the catalytic mechanism.^{24,25} Due to the high binding energy of the TS/TS-like

(23) Estiu, G. L.; Merz, K. M., Jr. *J. Am. Chem. Soc.* **2004**, *126*, 6932–6944.

(24) Wolfenden, R.; Snider, M. *J. Acc. Chem. Res.* **2001**, *34*, 938–945.

(25) Lee, J. K.; Houk, K. N. *Science* **1997**, *276*, 942–945.

(22) Lippard, S. J. *Science* **1995**, *268*, 996–997.

intermediate(s), the most proficient enzymes are more sensitive to reversible inhibitors that are designed to resemble them.²⁶

To mimic the active-site chemistry of urease, several molecular model systems have been synthesized, which were designed to evaluate the possible binding modes of urea as well as to carry out hydrolytic transformations at dinuclear nickel(II) cores that mimic the urease active site.^{27–40} The bidentate coordination of urea has been supported, in part, by the isolation of complexes such as $[L_2Ni_2(m-OAc)-(urea)](ClO_4)_2$ (L = pyrazolate derivative), where hydrogen bonding by the NH_2 groups to an oxygen atom of a bridging carboxylate was confirmed by structural analyses.³⁴ Further structural confirmation of urea bidentate coordination has been derived from the crystallographic analysis of triazacyclononane (TACN)/pyrazolate hybrid complexes.³¹ The pyrazolate-based dinickel complexes generally lead to ethanolysis of urea rather than hydrolysis³⁴ and constitute one of the most extensively studied families of bioinorganic urease mimics.^{31,34–39} Ethanolysis of urea at the dinickel center presumably takes place via nucleophilic attack of ethanol on coordinated urea. This mechanism has been also analyzed for the carboxylate-bridged dinickel(II) complexes $[Ni_2(Me_4-tpdp)(CH_3CO_2)(urea)]^{2+}$, where the reaction path is assumed to involve the simultaneous coordination of ethanol and the urea to the Ni centers.⁴¹ Complexes that promote the elimination of ammonia from coordinated urea are also known.^{37,42} It has been suggested, on the basis of the study of these complexes, that the hydrolysis of urea at a dinickel center proceeds through by initial elimination of ammonia from the coordinated urea molecule followed by hydrolysis of the resulting coordinated cyanate complex. This reaction pathway was observed in phthalazine–dinickel urease mimics^{28,29} and provides evidence for a mechanism that has long been considered an alternative pathway for the enzymatic hydrolysis of urea.^{43,44} To better analyze this mechanism, the influence of *N*-alkyl substitution of the coordinated urea has also been investigated.²⁸ The combination of kinetic data derived from the study of the alkylated and nonalkylated structures has provided valuable information through the identification of the reaction products associated with the different substitutions.

Nevertheless, the elimination pathway has not been as extensively studied as the hydrolytic one.^{10,45,46} For the latter, the participation of key residues in the reaction kinetics has been thoroughly discussed.^{7–13,20,21} A mechanistic analysis of the probable reaction intermediates that can be observed when the urea molecule, bonded to the dinickel–phthalazine ligand, is converted to acetonitrile would clearly help in furthering our understanding of the energetics of the elimination pathway.

It is clear, from the previous discussion, that there is a large amount of experimental information, derived from both structural biochemistry and bioinorganic studies, which could benefit from a theoretical analysis. Previous theoretical studies have mainly focused in the urease active site. The characteristics of the site,^{45,47} as well as the interaction with different inhibitors,^{10,46,48,49} have been analyzed by both quantum chemical and molecular mechanical approaches. Bioinorganic synthetic complexes are particularly relevant to study the active site of metalloenzymes, because they provide spectroscopic information against which theoretical results can be compared. We have chosen, for this study, the phthalazine–dinickel complexes, since they address the hydrolytic decomposition of coordinated urea. We have applied high-level quantum chemical methodologies to identify stable intermediates and transition-state structures, targeting a description of the lowest energy reaction pathway. Valuable experimental evidence was obtained from the analysis of the alkyl-substituted derivatives, which allows us to disregard several potential intermediates.²⁸ Nonetheless, they have been considered throughout in a comparative manner. Moreover, the favored mechanism we have identified is compared with what has been suggested to occur in the enzyme active site, mainly in relation to the participation of key residues of the protein as proton donors or acceptors.

Methodology

Each nickel ion contained in the phthalazine–dinickel complex contains two electrons, which have parallel unpaired spins (high-spin quintet state), defining a cation of charge +2. The antiferromagnetic coupling of the bridged dinickel(II) systems has been experimentally determined for μ -acetate complexes³⁴ and theoretically evaluated for model systems of the urease active site.⁴⁵ Dealing with open-shell transition metal complexes, we have chosen to use unrestricted density functional theory (UDFT) methods implemented in Gaussian 03.⁵⁰ DFT methods have been shown to reproduce the structural properties of

- (26) Phillips, L. M.; Lee, J. K. *J. Am. Chem. Soc.* **2001**, *123*, 12067–12073.
(27) Barrios, A. M.; Lippard, S. J. *J. Am. Chem. Soc.* **1999**, *121*, 11751–11757.
(28) Barrios, A. M.; Lippard, S. J. *Inorg. Chem.* **2001**, *40*, 1250–1255.
(29) Barrios, A. M.; Lippard, S. J. *J. Am. Chem. Soc.* **2000**, *122*, 9172–9177.
(30) Brown, D. A.; Errington, W.; Glass, W. K.; Haase, W.; Kemp, T. J.; Nimir, H.; Ostrovsky, S. M.; Werner, R. *Inorg. Chem.* **2001**, *40*, 5962–5971.
(31) Buchler, S.; Meyer, F.; Kaifer, E.; Pritzkow, H. *Inorg. Chim. Acta* **2002**, *337*, 371–386.
(32) Carlsson, H.; Haukka, M.; Nordlander, E. *Inorg. Chem.* **2002**, *41*, 4981–4983.
(33) Carlsson, H.; Latour, J. M.; Haukka, M.; Bousseksou, A.; Nordlander, E. *Inorg. Chem.*, submitted for publication.
(34) Konrad, M.; Meyer, F.; Jacobi, A.; Kircher, P.; Rutsch, P.; Zsolnai, L. *Inorg. Chem.* **1999**, *38*, 4559–4566.
(35) Meyer, F.; Hyla-Kryspin, I.; Kaifer, E.; Kircher, P. *Eur. J. Inorg. Chem.* **2000**, *2000*, 771–781.
(36) Meyer, F.; Jacobi, A.; Nuber, B.; Rutsch, P.; Zsolnai, L. *Inorg. Chem.* **1998**, *37*, 1213–1218.
(37) Meyer, F.; Kaifer, E.; Kircher, P.; Heinze, K.; Pritzkow, H. *Chem. Eur. J.* **1999**, *5*, 1617–1630.
(38) Meyer, F.; Konrad, M.; Kaifer, E. *Eur. J. Inorg. Chem.* **1999**, *1999*, 1851–1854.
(39) Meyer, F.; Pritzkow, H. *Chem. Commun.* **1998**, *1998*.
(40) Roecker, L.; Akande, J.; Elam, N.; Gauga, I.; Helton, B. W.; Prewitt, M. C.; Sargeson, A. M.; Swango, J. H.; Willis, A. C.; Xin, T.; Xu, J. *Inorg. Chem.* **1999**, *38*, 1269–1275.
(41) Yamaguchi, K.; Koshino, S.; Akagi, F.; Suzuki, M.; Uehara, A.; Suzuki, S. *J. Am. Chem. Soc.* **1997**, *119*, 5752–5753.
(42) Uozumi, S.; Funutachi, H.; Ohba, M.; Okawa, H.; Fenton, D. E.; Shindo, K.; Murata, S.; Kitko, D. *Inorg. Chem.* **1998**, *37*, 6281–6287.
(43) Fearon, W. R. *Biochem. J.* **1923**, *17*, 84–93.
(44) Mack, E.; Villars, D. E. *J. Am. Chem. Soc.* **1923**, *45*, 505–510.

- (45) Suarez, D.; Diaz, N.; Merz, K. M., Jr. *J. Am. Chem. Soc.* **2003**, *125*, 15234–15247.
(46) Zimmer, M. *J. Biomol. Struct. Dyn.* **2000**, *17*, 787–797.
(47) Manunza, B.; Deiana, S.; Pintore, M.; Solinas, V.; Gessa, C. *J. Mol. Struct. (THEOCHEM)* **1997**, *419*, 33–36.
(48) Manunza, B.; Deiana, S.; Pintore, M.; Gessa, C. *Soil Biol. Biochem.* **1992**, *31*, 789–796.
(49) Csiki, C.; Zimmer, M. *J. Biomol. Struct. Dyn.* **1999**, *17*, 121–131.
(50) Frisch, M. J.; Trucks, G. W.; Schlegel, H. B.; Scuseria, G. E.; Robb, M. A.; Cheeseman, J. R.; Montgomery, J. A., Jr.; Vreven, T.; Kudin, K. N.; Burant, J. C.; Millam, J. M.; Iyengar, S. S.; Tomasi, J.; Barone, V.; Mennucci, B.; Cossi, M.; Scalmani, G.; Rega, N.; Petersson, G. A.; Nakatsuji, H.; Hada, M.; Ehara, M.; Toyota, K.; Fukuda, R.; Hasegawa, J.; Ishida, M.; Nakajima, T.; Honda, Y.; Kitao, O.; Nakai, H.; Klene, M.; Li, X.; Knox, J. E.; Hratchian, H. P.; Cross, J. B.; Adamo, C.; Jaramillo, J.; Gomperts, R.; Stratmann, R. E.; Yazyev, O.; Austin, A. J.; Cammi, R.; Pomelli, C.; Ochterski, J. W.; Ayala, P. Y.; Morokuma, K.; Voth, G. A.; Salvador, P.; Dannenberg, J. J.; Zakrzewski, V. G.; Dapprich, S.; Daniels, A. D.; Strain, M. C.; Farkas, O.; Malick, D. K.; Rabuck, A. D.; Raghavachari, K.; Foresman, J. B.; Ortiz, J. V.; Cui, Q.; Baboul, A. G.; Clifford, S.; Cioslowski, J.; Stefanov, B. B.; Liu, G.; Liashenko, A.; Piskorz, P.; Komaromi, I.; Martin, R. L.; Fox, D. J.; Keith, T.; Al-Laham, M. A.; Peng, C. Y.; Nanayakkara, A.; Challacombe, M.; Gill, P. M.; Johnson, B.; Chen, W.; Wong, M. W.; Gonzalez, C.; Pople, J. A. *Gaussian*; Gaussian Inc.: Pittsburgh, PA, 2003.

several biologically interesting transition metal centers.^{51–54} Moreover, their validity in modeling ground-state properties is widely accepted.⁵¹

The dinuclear phthalazine complexes were subjected to energy minimizations using the B3LYP functional⁵⁵ with the double- ζ 6-31G* basis set⁵⁶ for nonmetal atoms and the Los Alamos effective core potentials (LANL2DZ)^{57,58} for the metal atoms (the mixed basis set will be denoted as LACVP*). The accuracy of the effective core potentials for Ni ions has been previously reported,⁴⁵ following a comparison of the geometries, energies, and charges for a series of Ni–L complexes (L = OH[−], H₂O, CH₃COO[−], etc.) when using the LACVP*, 6-31G*, and 6-311G** basis sets for Ni.

The structures that are shown in this paper are representative of the different steps involved in the postulated reaction pathways and have been fully optimized without imposed constraints. We report the structural parameters and associated energies for reactants, products, stable intermediates, and transition states. The search for stationary points on the potential energy surface utilized gradient-based algorithms and quadratic synchronous transit (QST2) approaches. Critical points have been further characterized by analytical computation of the harmonic frequencies at the same level of theory. A thermochemical analysis has been performed as a way to evaluate the free energy changes associated with the reaction, which becomes important when more than one species is involved. Solvent effects (aqueous solution), were included using an isodensity continuum polarizable model.⁵⁹ Atomic charges were computed according to the Merz–Kollman approximation,⁶⁰ at the same level of theory.

Results and Discussion

(1) Phthalazine Bridged Dinickel Complexes. The X-ray crystal structure of [Ni₂(μ -OH)(μ -H₂O)(bdptz)(urea)₂](ClO₄)₃, (bdptz = 1,4-bis(2,2'-dipyridylmethyl)phthalazine) shows a dinuclear nickel complex bridged by the phthalazine moiety of the bdptz ligand, a water molecule, and a hydroxide ion.²⁹ Each nickel atom is ligated to two pyridine donor arms from the ligand, and the pseudooctahedral coordination sphere of each nickel is filled by a urea molecule bound via its carbonyl oxygen atom.

Despite the rigidity of the phthalazine ligand, which is capable of keeping the Ni atoms at a distance close to that found in the urease active site (3.1 Å in the complex vs 3.5 Å in the enzyme active site), several conformations can be achieved by means of rotations around the Ni–O and the O–C bonds of urea. We have identified three conformers, very similar in energy, which involve different H-bonding patterns (see Figures 2 and 3). Hydrogen bond interactions can involve H donation from the bridging water to an amine nitrogen of urea (S1, Figure 2) or inverse H donation, from the amine group of urea to the bridging O. Moreover, for the second case, both of the ligated urea molecules can coordinate to the same bridging OH (S2a, Figure 3), or they can establish an inter-amide nitrogen N–H \cdots N hydrogen bond, while, at the same time, the acceptor amide

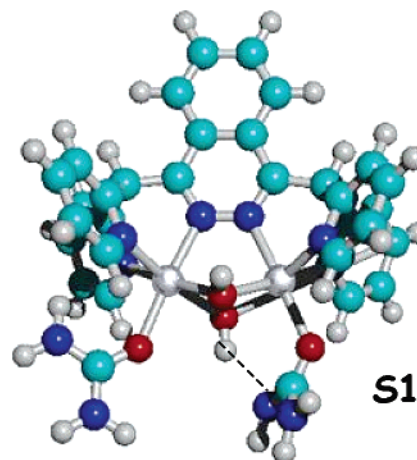


Figure 2. B3LYP/LACVP*-optimized structure of the less stable conformer of [Ni₂(μ -OH)(μ -H₂O)(bdptz)(urea)₂](ClO₄)₃ (bdptz = 1,4-bis(2,2'-dipyridylmethyl)phthalazine), associated with hydrogen bond donation from the inter-Ni water to one of the amido ends of the urea moiety.

nitrogen donates a hydrogen to the bridging OH (S2b, Figure 3). We predict that the second and third conformations are isoenergetic, while the first one is 12 kcal/mol higher in energy than the others. The second one was the one observed by the X-ray analysis: the urea molecule binds to Ni via its carbonyl group, while one amide nitrogen of each urea coordinates the intermetal OH through hydrogen bond donation.²⁹ The experimental and calculated values for relevant interatomic distances and planar angles are reported in Table 1 (Supporting Information), together with the geometric data determined for an isolated urea molecule by means of microwave spectroscopy.⁶¹ The interatomic distances do not deviate significantly after coordination. The analysis of the atomic charges, on the other hand, indicates a decrease of the negative charges on the carbonyl oxygen and amide nitrogens, an effect that is certainly triggered by coordination to the electropositive Ni centers. The overall charge on the urea moiety becomes 0.3e more positive after binding. The calculated stretching frequency for the C–O bond (1637 cm^{−1}) agrees with the experimental value derived from solid-state FTIR (1663 cm^{−1}), exhibiting a downshift from the value for isolated urea (1690 cm^{−1}).

In the experimentally observed structure (S2a), the slight conformational change in the urea moiety is indicative of an increased N lone pair back-donation, which decreases the C–N bond distance and increases the C–O one, with simultaneous planarization of the NH₂ groups due to the augmented sp² character of the nitrogen centers (see Table 1, Supporting Information). A similar coordination mode has been found in a recent theoretical analysis of the interaction of urea with cluster models of the urease active site, comprising both coordination of the urea carbonyl O to one Ni atom and H-bond donation from the amine moiety to the bridging OH.⁴⁵ This mode of binding facilitates the ability of the bridging hydroxide to attack the carbonyl carbon atom to give a tetrahedral intermediate which follows the decomposition mechanism that is the most widely accepted (see Figure 4).⁶

According to the proposal by Benini et al.,⁸ the bridging hydroxide group can also act as the general acid donating its proton to the leaving ammonia molecule which, in turn, interacts

(51) Chang, C. H.; Boone, A.; Bartlett, R. J.; Richards, G. J. *Inorg. Chem.*, in press.

(52) Siegbahn, P. E. *Curr. Opin. Chem. Biol.* **2002**, *6*, 227–235.

(53) Harris, D. L. *Curr. Opin. Chem. Biol.* **2001**, *5*, 724–735.

(54) Ghosh, A.; Steene, E. J. *Biol. Inorg. Chem.* **2001**, *6*, 739–752.

(55) Becke, A. D.; Yarkony, D. R. *Modern Electronic Structure Theory*, Part II; World Scientific: Singapore, 1995.

(56) Hehre, W. J.; Radom, L.; Schleyer, P. v. R.; Pople, J. A. *Ab Initio Molecular Orbital Theory*; Wiley: New York, 1986.

(57) Hay, P. J.; Wadt, W. R. *J. Chem. Phys.* **1985**, *82*, 270–283.

(58) Wadt, W. R.; Hay, P. J. *J. Chem. Phys.* **1985**, *82*, 284–298.

(59) Foresman, J. B.; Keith, T. A.; Wiberg, K. B.; Snoonian, J.; Frisch, M. J. *J. Phys. Chem.* **1996**, *100*, 16098.

(60) Besler, B. H.; Merz, K. M., Jr.; Kollman, P. A. *J. Comput. Chem.* **1990**, *11*, 431.

(61) Rousseau, B.; Van Alsenoy, C. *J. Phys. Chem. A* **1998**, *102*, 6540–6548.

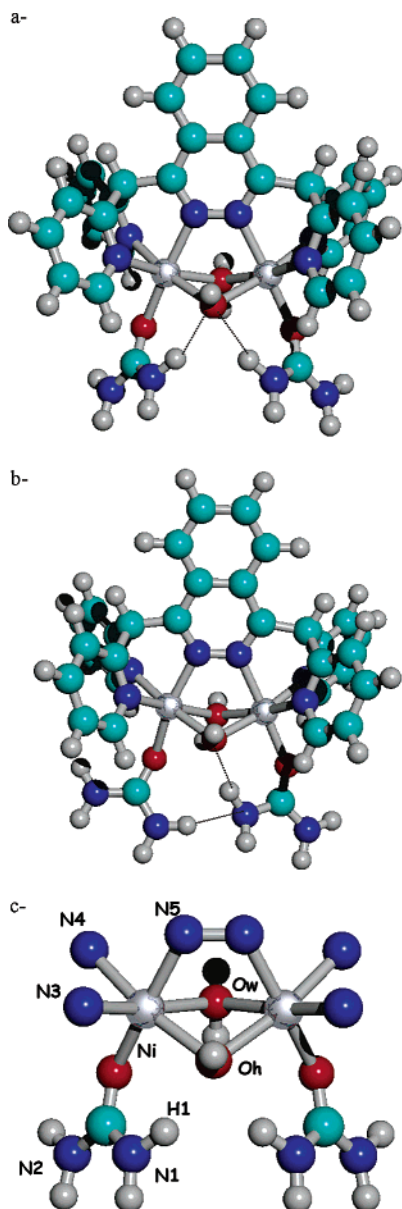


Figure 3. B3LYP/LACVP*-optimized structure of the low-energy conformers of $[\text{Ni}_2(\mu\text{-OH})(\mu\text{-H}_2\text{O})(\text{bdptz})(\text{urea})_2](\text{ClO}_4)_3$ ($\text{bdptz} = 1,4\text{-bis}(2,2'\text{-dipyridylmethyl})\text{phthalazine}$): (a) s2a Coordination of both amido ends to the bridging OH; (b) s2b hydrogen bond coordination between the amido ends of two different urea molecules as well as a hydrogen bond interaction to the bridging OH; (c) a portion of the molecule in which the aromatic phthalazine ligand has been deleted. The atom names used in the text and in the tables (see Supporting Information) are indicated.

with His320. The $\text{p}K_{\text{a}}$ for hydroxide deprotonation is probably reduced by coordination to the Ni atoms, and, indeed, a value of around 9 has been estimated.⁶² Prior to proton transfer, the hydroxyl oxygen atom is proposed to coordinate with the carbonyl C atom of urea, which is proposed to further decrease the $\text{p}K_{\text{a}}$. Proton abstraction is thought to be aided by the carboxylate group of Asp363, which is bound to Ni2. This proposal has the added benefit that the charge of the active site cluster does not change. This mechanism is more compatible with conformer S1, shown in Figure 1, which is not the one derived from X-ray analysis. In this case, H-bond donation

involves the Ni-bridging water molecule instead of an OH group. The process triggers a change in the hybridization of the acceptor amide nitrogen of urea. The resulting sp^3 contribution is supported by the pyramidalization of the amide nitrogen group (the sum of the H–N–H angles around the N atom is 339°) and also by the elongation of the CN bond to 1.40 \AA . The other amide nitrogen retains the characteristics previously described for S2a. Urea elimination from this conformer has been theoretically evaluated, on the assumption that the S1→S2a interconversion is not energetically demanding.

Alternatively, Karplus et al. suggested that protonation occurs via the general acid His320 (i.e., His320 is protonated in the native form of the enzyme; see Figure 4).⁶ To account for this possibility, we have considered the possible participation of an external agent (residue or solvent) in the design of our postulated reaction paths.

(2) Analysis of Possible Reaction Pathways. (2.1) NH_3 Release after Intramolecular Proton Transfer. On the basis of the modest energy differences between the structures shown in Figures 2 and 3, which allows for their mutual interconversion, we must consider all of them as being potentially responsible for NH_3 release after intramolecular hydrogen transfer. S2a can react via hydrogen transfer involving both amide nitrogen atoms of a single urea moiety, while S2b is more prone to proton transfer between the amide nitrogens from the two different urea molecules that are already coordinated. However, experimental analysis of several complexes, closely related to those shown in Figures 2 and 3, does not favor the latter because it was shown that NH_3 is also released when an acetonitrile molecule replaces one of the urea ligands bonded to one of the nickel atoms of the complex (see Figure 5). This observation rules out inter-urea H-transfer as a necessary step in the elimination mechanism. Moreover, the intermediate that would result from this transfer (a protonated amide nitrogen group on one of the urea molecules and a deprotonated one on the other) is not computed to be stable, but collapses directly to S2b. Additional valuable information can be extracted from analysis of several derivatives of the dinickel–phthalazine complex, arising from *N*-alkyl substitution of the ligated urea molecules. It has been shown that *N*-methylurea and *N,N*-dimethylurea derivatives release measurable amounts of the corresponding alkylamine and cyanate ion from decomposition, but no such products were observed with *N,N*-dimethylurea or tetramethylurea. The only decomposition pathway available for these products is hydrolysis. These observations offer a clear indication that two hydrogen atoms should be attached to the urea nitrogen atom that is H-bonded to the inter-Ni OH (H1 and H2, see Figure 3).

Utilizing the previously discussed experimental evidence and the results of recent calculations on the kinetics of the solution-phase decomposition of urea,²³ we initially analyzed the reaction pathway involving an intramolecular proton-transfer mechanism restricted to a single urea molecule.

As a first step we considered the decomposition pathway traditionally accepted for the urea elimination reaction, originally described in the early 1950s.^{63–65} In light of this, we have evaluated the energy associated with intramolecular proton

(62) Basolo, F.; Pearson, R. G. *Acid-Based Properties of Complex Ions. Mechanisms of Inorganic Reactions*; Wiley: New York, 1967.

(63) Laidler, K. J.; Hoare, J. P. *J. Am. Chem. Soc.* **1950**, *72*, 2489–2494.

(64) Shaw, W. H.; Bordeaux, J. J. *J. Am. Chem. Soc.* **1955**, *27*, 4729–4733.

(65) Shaw, W. H. R.; Walker, D. G. *J. Am. Chem. Soc.* **1958**, *80*, 5337–5342.

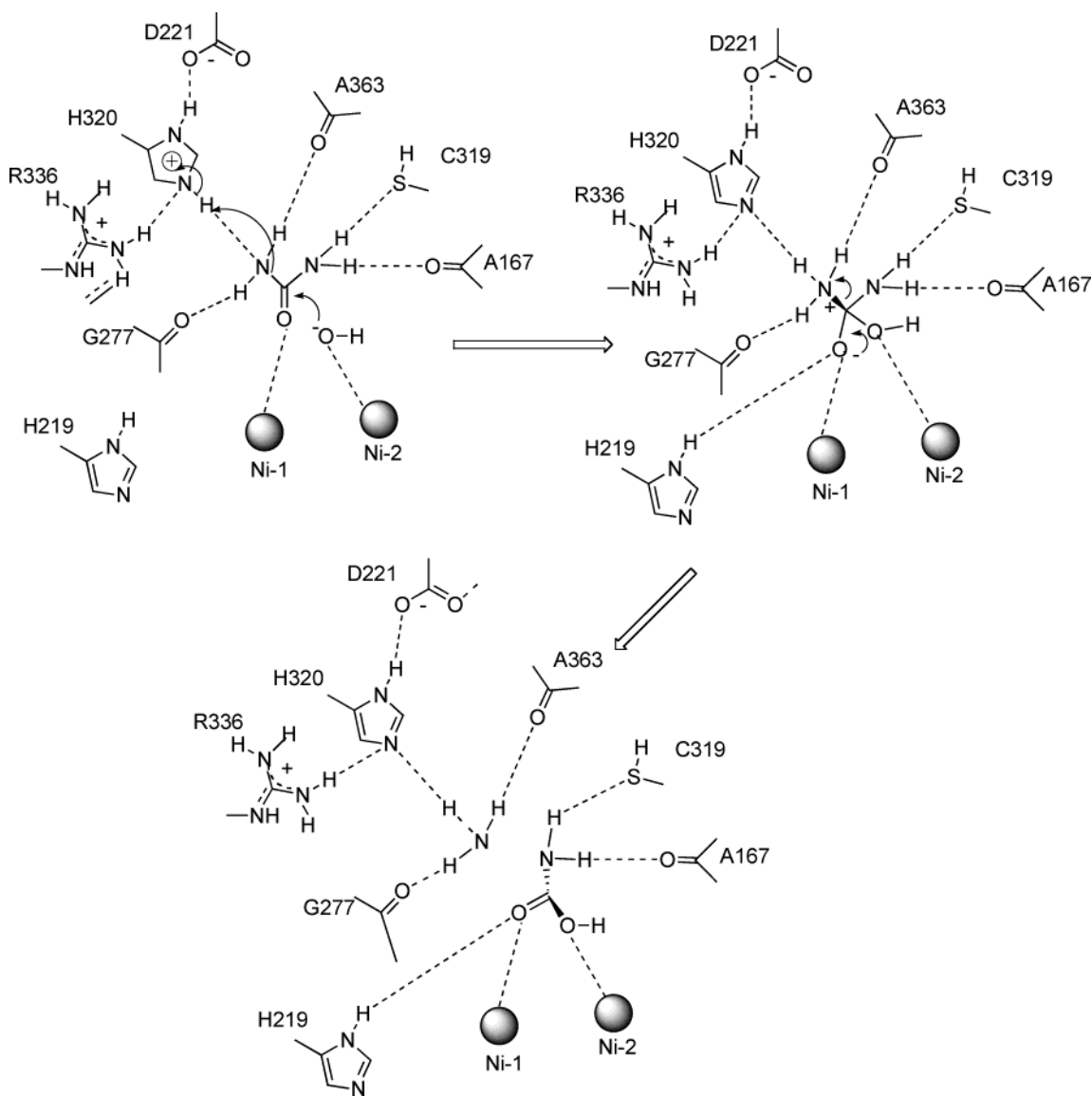


Figure 4. Structurally detailed mechanism for urease catalysis as proposed by Karplus and Hausinger. The reaction proceeds through a tetrahedral intermediate that gives carbamic acid after NH_3 release.

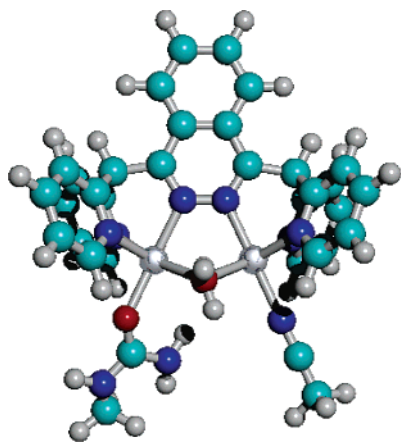


Figure 5. LACVP*-optimized structure of $[\text{Ni}_2(\mu\text{-OH})(\mu\text{-H}_2\text{O})(\text{bdptz})(N\text{-methylurea})(\text{CH}_3\text{CN})](\text{ClO}_4)_3$ (bdptz = 1,4-bis(2,2'-dipyridylmethyl)phthalazine).

transfer between the amide nitrogens of one of the ligated urea molecules. This reaction pathway proceeds through a planar four-center transition state (TSa1, see Figure 6), which raises

the energy of the system to 55 kcal/mol. In this optimized structure NH_3 formation is advanced, which elongates the C–N bond to 1.53 Å. The first stable intermediate (Ia1, Figure 6) is 23 kcal/mol higher in energy than the initial complex. In this structure, an amide hydrogen (H2, Figure 3) has been completely transferred, resulting in a NH_3 group singly bonded to the carbon atom of a Ni-coordinated cyanic acid. For this intermediate species, the H-bond pattern associated with S2b is favored by 7 kcal/mol over the one associated with S2a. From Ia1, the release of NH_3 is not favored, because it leads to products (NH_3 and the protonated acetonitrile complex) that are 16 kcal/mol less stable than the original reactants. Alternatively, the ammonium ion (NH_4^+) can be released yielding Pa2 (Figure 6) as product. The protonation of the departing NH_3 by the hydrogen atom, H1, requires the rupture of the H1–Oh hydrogen bond. This proceeds via TSa2, (see Figure 6), which is 23 kcal/mol uphill. In TSa2, the NH_3 moiety is far enough from the C atom, which allows it to attain the sp hybridization pattern characteristic of a linear OCN arrangement (see Table 2, Supporting Information).

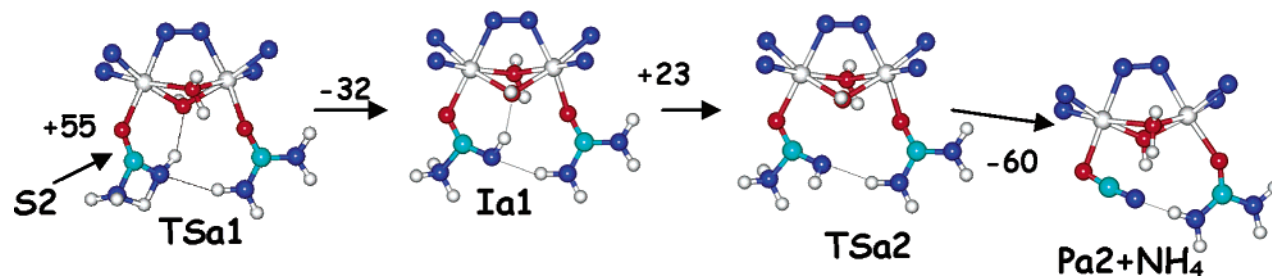
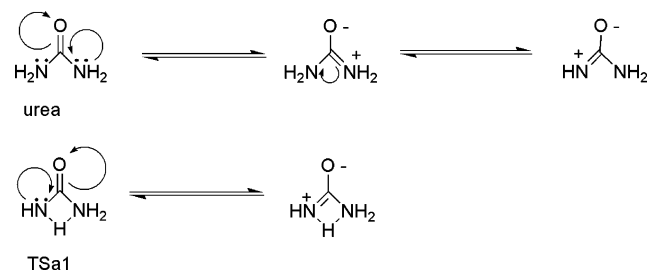


Figure 6. B3LYP/LACVP*-optimized geometries of the intermediate (Ii), transition-state (TSi), and product (Pai) structures involved in the intramolecular proton-transfer elimination reaction pathway. The phthalazine ligand has been partially deleted for clarity. Differences in gas-phase free energy (ΔG , kcal/mol) between consecutive steps are given.

Scheme 1



The overall process is uphill in energy by 55 kcal/mol, with the activation barrier defined by the four-center TS1a. This barrier height is not attainable under the experimental conditions employed. In TS1a, the resonance stabilization of urea is clearly disrupted. The hybridization on the amide N atoms changes from a mixed sp^2 - sp^3 electronic configuration to sp^2 hybridization on the H-donor atom and sp^3 on the H-acceptor atom. This change is reflected in the respective decrease and elongation of the associated C–N bonds (see Table 2, Supporting Information). In TS1a, the migrating proton (H2, see Figure 3) is at the midway point between the two amide nitrogen atoms. To attain this coordination, the N1CN2 angle decreases from 113 to 94°, at the expense of an increase of the OCN1 angle to 140°. The structure can be described as a distorted isocyanic acid, where ammonia is coordinated to the C atom. In this way, the electron delocalization, which in the urea molecule extends over four atomic centers, is restricted to three atoms in TS1a. This effect is shown in Scheme 1 for an isolated urea molecule.

(2.2) Water-Assisted Intramolecular Proton Transfer.

According to the urease mechanism proposed by Karplus,⁶ ammonia elimination can be assisted by protonation of the amide nitrogen group carried out by a protein residue or a water molecule. Despite the different environments of urea in the urease active site and in the phthalazine complex, we studied this possibility by modeling the interaction of a water molecule with one of the Ni-coordinated urea molecules. The kinetics of urea decomposition promoted by the dinickel model complex has been experimentally studied by the method of initial rates, using acetonitrile solutions of different dilutions; hence, water could be a significant factor in catalysis.^{28,29}

By studying this reaction path, we are extending previous results on the solution-phase decomposition of urea.²³ The most favored coordination mode for water involved H-bond donation from the amide nitrogen groups to the oxygen atom in water (S3, see Figure 7), which decreases the energy by 17.1 kcal/mol, relative to the separated species. When entropic contributions are considered, the stabilization is reduced to 6.5 kcal/mol. Moreover, inclusion of solvation effects predicts that the

separated and coordinated species are isoenergetic. A similar description was found in a theoretical study of the aqueous phase decomposition of urea.²³ The dinickel phthalazine ligand, bound to urea, stabilizes water coordination as a result of the increased acidity of the amide hydrogen atoms due to the electropositive metal centers. Furthermore, the hydrogen atoms on the amide nitrogen atoms located within the same urea molecule show differential nucleophilic character, because one is H-bonded to the bridging OH group. This results in a six-membered hydrogen bonding pattern where the water molecule is associated with the NH_2 group that is not interacting with OH (see S3, Figure 7, and Table 3 of Supporting Information). The second urea molecule is H-bonded to the NH_2 group that is associated with the bridging OH group.

The hydrogen bond pattern of the water–urea complex facilitates the intermolecular proton-transfer mechanism. The first intermediate identified is 29 kcal/mol higher in energy than the urea–water complex (Ib1, see Figure 7). This intermediate is reached via the concerted transfer of two hydrogen atoms: the first one, H2, belonging to the urea amide group that is interacting with the bridging OH (see Figure 3) to the incoming water, and the second one, belonging to the water molecule, which donates a proton (WH, see Figure 7) to the NH_2 that will ultimately be released as NH_3 . The resulting hydrogen bond pattern defines a six-membered ring stabilized through N–H and O–H hydrogen bonds.

A second intermediate (Ib2, see Figure 7), which is very close to the products, involves a reverse H-bond coordination of the urea moieties to Oh, relative to Ib1 (the coordination is defined by the donation of H3, instead of H1, to Oh). In this second intermediate the complete release of ammonium and water has almost been achieved. The associated TS structure (TSb2, see Figure 7) is lower in energy than the first one and does not determine the activation energy.

The release of NH_3 and water leaves isocyanic acid coordinated to Ni (Pa1, see Figure 7). The resulting product is stabilized by H-bonds between the remaining urea moiety to the bridging OH. The reaction products are further stabilized as ionic species (Pa2, see Figure 6), due to the influence of the positively charged Ni atom, which decreases the pK_a of the cyanic acid bound to it.

The transformation from TSb1 and the noncharged products (Pa1 and NH_3) involves structures that are almost isoenergetic, with the driving force being the formation of NH_4^+ and Ni-coordinated cyanate. However, the protonation of NH_3 by the Ni-coordinated cyanic acid requires prior breaking of the N1–H1–Oh hydrogen bond, following a mechanism that proceeds through intermediate Ib3 (see Figure 7), which is 8 kcal/mol

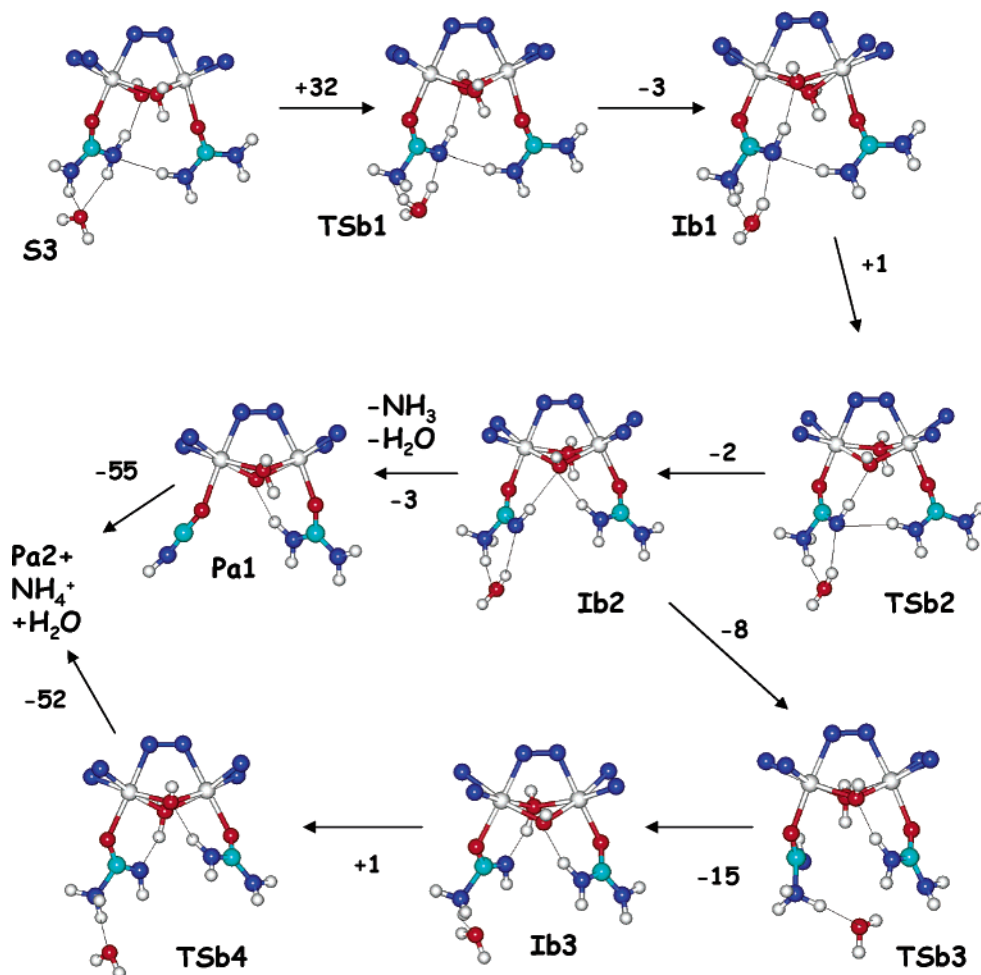


Figure 7. B3LYP/LACVP*-optimized geometries of the intermediate (Ii) and transition-state (TSi) structures involved in the water-assisted elimination reaction of urea. The phthalazine ligand has been partially deleted for clarity. Differences in gas-phase free energy (ΔG) between consecutive steps are given.

more stable than Ib2. The activation energy for this step of the reaction (8 kcal/mol) originates in the torsional deformation of the OCN1H1 angle (see Table 3) and the subsequent rupture of the H-bond between N1 and Oh (see TSb3, Figure 7). Finally, we note that a broad range of hydrogen bond interactions are available that can stabilize the various intermediate and transition-state structures, thereby defining different possible reaction paths leading ultimately to the same products. The possible coordination modes involve, among others, Oh–H1, Oh–H3, H1–N6, H3–N1, H2–Ow, and H4–Ow bond formations. The multiplicity of available H-bond patterns makes it difficult to elucidate which are the most favored, but, clearly, the addition of water greatly facilitates the overall reaction.

(2.3) NH₃ Release from Conformer S1. To assess the ability of S1 to participate in the NH₃ elimination mechanism, the energy involved in the interconversion between S2a and S1 was evaluated. The process proceeds through a transition-state structure (TS0, see Figure 8), which is very close to S1, with an activation energy (13 kcal/mol) that is similar to the energy difference between the two conformers (12 kcal/mol). From S1 an elimination mechanism can be constructed that can compete with the water-assisted intramolecular proton transfer.

From S1, proton transfer from the bridging water molecule to an amide nitrogen of the urea molecule gives the structure TS_c1 (see Figure 8) after rotation around the C–O bond of the

urea moiety. A 120° rotation positions the unprotonated amine group of the urea moiety in an orientation that allows H-bond donation to the inter-Ni OH in the transition state (see TS_c1, Figure 8), with associated N–O and O–H distances of 2.55 and 1.55 Å, respectively. From TS_c1, completion of the proton transfer generates a stable intermediate (Ic1), which regenerates the geometry of the dinickel center, while concomitantly decreasing the energy by 8 kcal/mol. In Ic1, the C–N(H₃) distance is elongated to 1.64 Å, and the H atom of the NH group points toward the N atom of NH₃. This configuration facilitates the release of NH₄⁺, which then generates Pa₂.

Although this reaction has an activation energy close to the one associated with the water-assisted elimination reaction (35 kcal/mol), the mechanism that proceeds through S1 is in disagreement with available experimental evidence. From the study of alkyl-substituted urea–phthalazine complexes,²⁸ it is known that *N*-methylurea and *N,N*-dimethylurea produce the corresponding alkylamine and the cyanate ion. Moreover, the results of both X-ray crystallography and our own calculations (data not given) indicate that the alkyl-substituted end of urea would point away from the bridging OH, as shown in Figure 5. For this geometry, proton transfer from the Ni-ligated water to the coordinated methylurea would not release methylamine but ammonium. Moreover, rotation around the C–O bond would similarly not be favored. On the basis of this, we suspect that

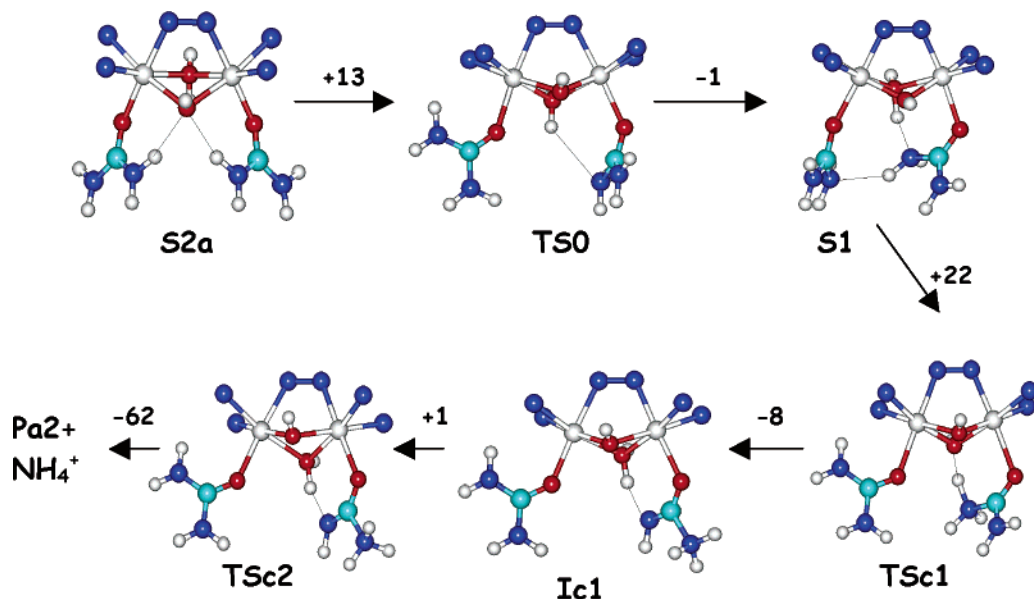


Figure 8. B3LYP/LACVP*-optimized geometries of the intermediate (Ii) and transition-state (TSi) structures involved in the elimination reaction proceeding through NH_3 release from the conformer S1. The phthalazine ligand has been partially deleted for clarity. Differences in the gas-phase free energy (ΔG , kcal/mol) between consecutive steps are given.

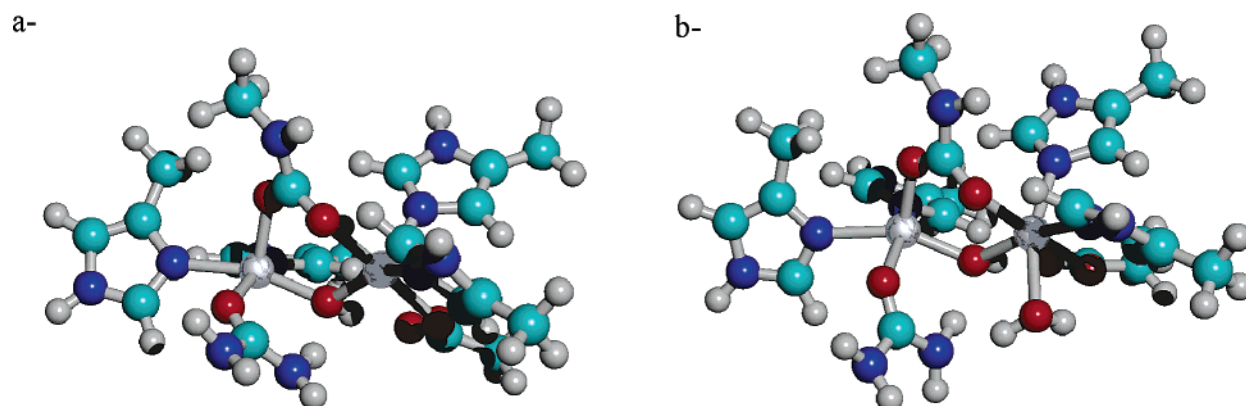


Figure 9. B3LYP/LACVP*-optimized geometries of urea-bonded cluster models of the urease active site (from ref 44). (a) Urea coordination displaces the Ni-bound water molecules in the active site of native urease. (b) A water molecule bound to the second Ni atom is retained after urea coordination.

this mechanism is not representative of the elimination reaction pathway for all of the phthalazine ligands that have been experimentally analyzed.

(3) Discussion. The interaction of urea with urease has been examined theoretically by several groups; for example, Zimmer and Csiki have used molecular mechanics methods to study substrate and inhibitor binding to urease,^{46,49} while Musiani et al. have used the Dock program to dock substrate and inhibitors into the urease active site.¹⁰ More recent quantum chemical calculations have identified stable coordination geometries for the urease–urea complex that strongly resemble the one experimentally found for the phthalazine-bridged dinickel–diurea complex.⁴⁵ The most stable coordination modes (Figure 9) are associated with monodentate binding of urea to the dinickel clusters, in which the carbonyl group of the urea molecule coordinates to the Ni atom, displacing a water molecule found in the native protein. The structure is further stabilized by hydrogen bond donation of one amino end of urea to the bridged hydroxide. The water molecule bound to the second Ni atom can be either retained or not (see Figure 9a,b, respectively). When retained, it contributes to the bonding of urea by establishing an H-bond with one amino end, resembling

the coordination of the second urea in Sb2. The conversion of these structures, following a mechanism similar to the one proposed for urease (see Figure 4),⁶ involves nucleophilic attack of the bridging OH on the carbonyl carbon, which generates a bidentate tetrahedral intermediate after loss of a water molecule from Ni2. This mechanism was not observed for the phthalazine complexes, because the rigidity of the dinickel cluster impedes attack by the bridging hydroxide ion on the carbonyl carbon atom of urea. The alternate reaction pathway found for the phthalazine complexes involves hydrolysis of urea to ammonia and carbon dioxide via a two-step process requiring the initial elimination of ammonia from the coordinated urea molecule and the further hydrolysis of the resulting cyanate ion by an external water molecule. The mechanistic analysis presented herein focused on the first step of this reaction.

The energy profiles for the analyzed mechanisms show that the release of NH_3 from urea cannot arise from an intramolecular proton transfer within a urea moiety, because the four-center transition-state structure (TSa1, Figure 6) increases the energy of the system by 55 kcal/mol. The stability of the water–urea adduct when coordinated to the phthalazine complexes results from the increased acidity of the hydrogen bond to the amide

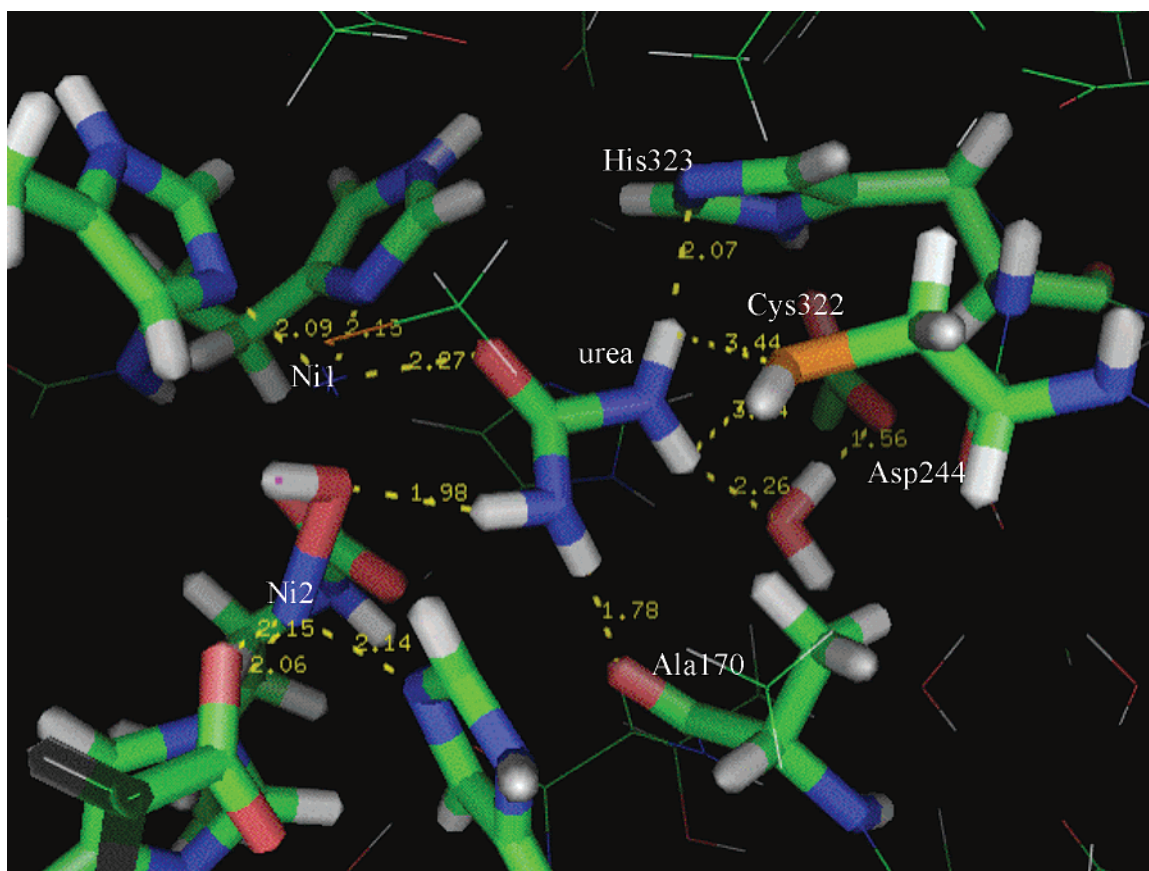


Figure 10. Coordination of urea to the active site of urease, after 2 ns MD simulation. The initial model has been built through urea docking to the active site of DAP-inhibited *B. Pasteurii* (PDB code 3UBP). H-bond coordination to key residues of the mobile flap are shown, as well as the interactions with the bridging OH.

nitrogen atoms (intramolecular hydrogen bonding), triggered by urea coordination to the positively charged Ni ions. This effect is also present in the enzyme active site and facilitates the stabilization of H-bond interactions between urea and key residues of the protein.

The assistance of a water molecule to lower the activation energy for the elimination reaction in these clusters resembles the role of His320 (residue numbering as in 1KAU) in urease. This residue, according to the mechanism proposed by Karplus et al.,⁶ helps in the release of NH_3 through the protonation of urea at the nitrogen atom that is pointing away from the bridging OH (see Figure 4). Thus water can be considered as playing the role of a key residue located on the mobile flap of urease, which is thought to actively participate in hydrolytic decomposition. The modeling of a water molecule as part of our proposed mechanism is supported by the results of MD simulations of the urea–urease system, which, have shown that water molecules, as well as protein residues, can be involved in H-bonding to the nitrogen of urea (see Figure 10).

Our MD simulations also favor a coordination geometry stabilized by H-bond donation from a urea nitrogen atom to the bridging OH (see Figure 10). This coordination mode resembles the one observed for the phthalazine complexes (see Figure 3).²⁹ Although we have previously predicted (for the aqueous-phase urea elimination reaction)²³ that this reaction is likely to proceed through a tetrahedral-intermediate-mediated mechanism, a alternative mechanism would involve the release of NH_3 , generating a Ni-coordinated cyanic acid that can be further hydrolyzed to carbamic acid. This elimination mecha-

nism may be favored in the phthalazine complexes, due to the relative rigidity of the central Ni–OH–Ni moiety. In the urease active site, on the other hand, elimination can be facilitated by initial transfer of the hydrogen bound proton to the bridging OH, followed by the release of ammonium after the protonation of the second amide nitrogen of urea by a nearby protein residue or solvent molecule, as shown in Figure 11. The resulting Ni-coordinated water can then be involved in the hydrolytic transformation of cyanic acid to carbamic acid.

For the case of unsubstituted urea, the mechanism represented in Figure 8 may be considered the favored pathway for the elimination reaction, as it does not need the assistance of a water molecule. Nevertheless, in the enzyme active site, the inter-Ni water molecule is thought to be as a hydroxide ion (based on an analysis of the pK_a).⁸ Hence, we do not predict that the mechanism represented in Figure 8 is a good model for the enzymatic reaction.

Conclusions

In this paper we report a comprehensive study of the possible reaction pathways for the decomposition of urea facilitated by the phthalazine ligand system, which is a bioinorganic model for the active site of urease. We employed computational methodologies to analyze equilibrium geometries, electronic properties, and energies for a series of intermediate structures and transition states.

From a comparison of different possible reaction mechanisms, we predict that a water molecule participates in the reaction,

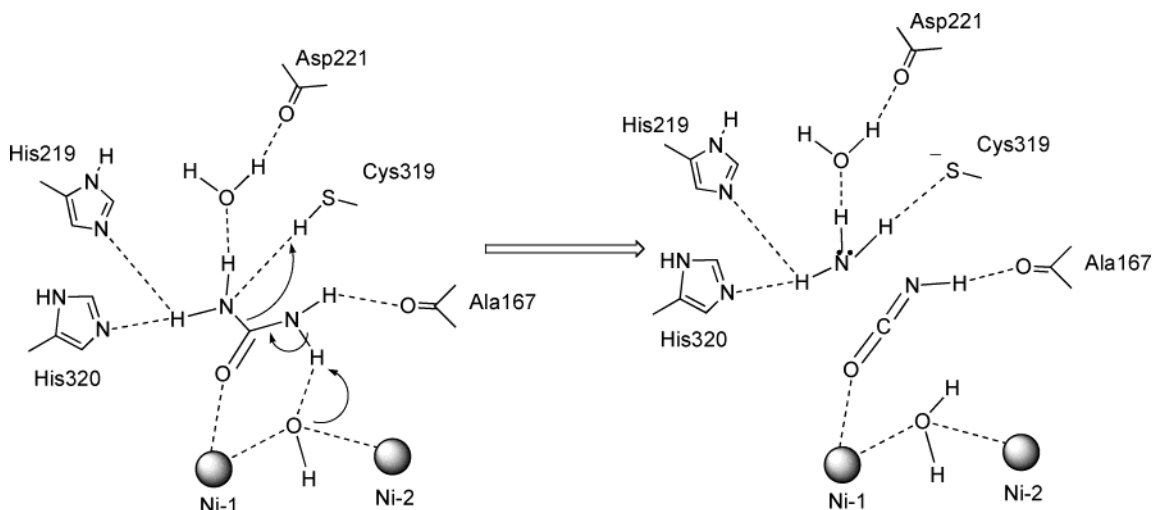


Figure 11. Structurally detailed mechanism for the urea elimination reaction catalyzed by urease proceeding via cyanic acid. The remaining Ni-bound water molecule can facilitate the hydrolysis to carbamic acid.

by facilitating the protonation of an amide nitrogen of urea that is subsequently released as NH_3 . This water molecule resembles the role of key residues (e.g., His320) in the enzyme active site, which hydrogen bond the amide nitrogens of urea. In both the enzyme and the phthalazine system intra- and intermolecular hydrogen bonding was enhanced by the increased acidity of the amide hydrogen atoms, triggered by coordination of urea to the positively charged Ni ions.

The coordination mode of urea, experimentally observed for the phthalazine complexes, and theoretically reproduced by us, indicates the presence of a hydrogen bond linking an amide nitrogen to the bridging OH. This coordination is also favored by MD simulations of the urea–urease system and possibly defines the initial step of a catalyzed elimination mechanism that generates carbamic acid after the hydrolysis of cyanic acid, which was formed in the first stage of the reaction. According to preliminary results of MD simulations, this two-step mechanism could occur in both the phthalazine model systems and in the enzyme active site.⁶⁶ On this basis, we postulate that the elimination mechanism (Figure 11) can compete with the

hydrolytic one (Figure 4) for the urease-catalyzed urea decomposition.

The hydrolytic decomposition of urea in the urease active site has been extensively studied. The likely formation of a tetrahedral intermediate in the reaction pathway is generally accepted and has been supported by the bidentate coordination mode of DAP to the urease active site.⁸ Nevertheless, there is no definitive evidence ruling out the possibility of a transient nickel-bound cyanate intermediate in urease. Such an intermediate would be consistent with the results of the calculations presented here, with preliminary MD simulations⁶⁶ and with the experimental work on which this study has been based.

Acknowledgment. We thank the National Center for Supercomputer Applications (NCSA) and Pittsburgh Supercomputer Center (PSC) for generous allocations of supercomputer time. We also thank the NIH for support via Grant GM066859.

Supporting Information Available: Tables showing relevant structural parameters. This material is available free of charge via the Internet at <http://pubs.acs.org>.

(66) Estiu, G. L.; Merz, K. M., Jr. Manuscript in preparation.